

# Truncated spherical-wave basis set for first-principles pseudopotential calculations

**B Monserrat and P D Haynes**

Department of Physics, Blackett Laboratory, Imperial College London, Exhibition Road, London SW7 2AZ

E-mail: [p.haynes@imperial.ac.uk](mailto:p.haynes@imperial.ac.uk)

**Abstract.** Analytic results for two- and three-centre integrals are derived for the truncated spherical-wave basis set designed for first-principles pseudopotential calculations within density-functional theory. These allow the overlap, kinetic energy and non-local pseudopotential matrix elements to be calculated efficiently and accurately. In particular, the scaling of the computational effort with maximum angular momentum component is dramatically improved and the projection method takes full account of the discontinuities in the basis functions arising from their localisation within spherical regions.

PACS numbers: 71.15.Ap

Submitted to: *J. Phys. A: Math. Theor.*

## 1. Introduction

Density-functional theory (DFT) is currently the method of choice for first-principles simulations of many materials due to the balance that it achieves between two competing requirements: on the one hand, a sufficiently accurate treatment of electron correlation for many purposes; on the other, a relatively modest computational cost that allows simulations of a few hundred atoms to be performed routinely. The plane-wave pseudopotential (PWP) method [1] is the workhorse for materials simulation based on DFT because of the simplicity of the plane-wave basis set that can be improved systematically using a single parameter, the energy cut-off  $E_{\text{cut}}$ ; the efficiency with which the operation of the Hamiltonian can be performed using fast Fourier transforms; and the use of the pseudopotential approximation to reduce the size of basis set required.

In common with all traditional implementations of DFT, the PWP method scales asymptotically in proportion to the cube of the system-size, as quantified for example by the number of atoms  $N$ , due to the orthogonality constraint on the single-particle wave-functions. Although this  $O(N^3)$  scaling compares favourably with correlated wave-function methods, it still limits the maximum system-size accessible to DFT and slows the rate at which improvements in computer performance can increase that limit. Over the last two decades there has therefore been much interest in the development of linear-scaling or  $O(N)$  methods for DFT [2]. For materials with a band gap, i.e. semiconductors and insulators, these methods exploit the nearsightedness of many-particle quantum mechanics that leads to the spatial localisation of quantities such as the Wannier functions and density-matrix [3]. Hence local orbitals play a fundamental role in the description of the electronic structure within linear-scaling methods.

The plane-wave basis set as originally conceived is incompatible with linear-scaling methods since basis functions that extend over the entire simulation cell cannot sensibly be used to expand local orbitals (although basis sets equivalent to a set of plane-waves [4] have been used successfully to optimise local orbitals [5] with plane-wave accuracy [6]). Localised basis sets employed in linear-scaling methods fall into two categories. Atomic-like orbitals e.g. Gaussian type orbitals [7], Slater-type orbitals [8] and numerical atomic orbitals [9] are relatively small in size. Basis sets consisting of larger sets of primitive functions e.g. splines [10], Lagrange functions [11] and real-space grids [12] have the advantage that they may be refined systematically. The localised spherical-wave basis set was proposed for linear-scaling methods [13] and successfully demonstrated in both  $O(N^3)$  [14] and  $O(N)$  [15] schemes. The rationale for this choice of basis is to obtain a set of localised functions that still retain some of the advantages of plane-waves, such as systematic control (in principle via the same single parameter  $E_{\text{cut}}$ ) and suitability for use in tandem with the pseudopotential approximation.

Analytic results for the two-centre overlap and kinetic energy matrix elements have previously been derived [13] that enhance the accuracy and potentially the performance of calculations employing spherical-waves. However this approach suffers from very poor scaling with the maximum angular momentum  $\ell_{\text{max}}$  included in the basis – typically

$\ell_{\max}!$  scaling – that increases the computational cost and in practice restricts  $\ell_{\max}$  to three at most. A projection method has also been outlined for treating the non-local pseudopotential matrix elements without the need for the Kleinman-Bylander separation [16] which did not however account for the discontinuity of the basis functions caused by localisation.

This paper revisits the previous analysis and addresses both deficiencies. Section 2 defines and motivates the localised spherical-wave basis set. In section 3 an approach is presented that leads to analytic results for the overlap and kinetic energy matrix elements whose implementation scales as  $\ell_{\max}^6$ . In section 4 the projection of basis functions localised within one sphere onto another is treated taking all terms into account and leading to an alternative method for the calculation of two-centre integrals and a particularly simple result (22) for the kinetic energy matrix elements. In section 5 particular examples of matrix elements are calculated by both methods and compared against numerical results. The computational costs of both methods are compared. Finally in section 6 methods for tackling three-centre integrals are presented.

## 2. Localised spherical-waves

The pseudopotential approximation combines the strong nuclear Coulomb potential and core electrons to produce a much weaker energy-dependent non-local potential with smooth valence wave-functions that lack the high frequency oscillations in the core region originally required for orthogonality. The choice of a plane-wave basis is justified by viewing this ionic potential as a perturbation of the free electron system whose Fourier transform decays rapidly as the wave-vector  $\mathbf{q}$  increases.

In deriving a localised basis set suitable for calculations within the pseudopotential approximation, it is therefore desirable to retain a connection with plane-waves by seeking solutions of the same free electron Schrödinger equation, the Helmholtz equation

$$\left(\nabla^2 + q^2\right) \psi(\mathbf{r}) = 0, \quad (1)$$

here written in Rydberg atomic units where the energy  $E = q^2$ . Plane-waves  $\exp(\mathbf{i}\mathbf{q} \cdot \mathbf{r})$  arise when periodic boundary conditions are applied, and the basis set is truncated by including only those for which  $q^2 < E_{\text{cut}}$ . Suppose instead that homogeneous Dirichlet boundary conditions are applied on the surface of a sphere of radius  $a$ , centred on the origin. The solutions take the form of truncated spherical-waves

$$\psi(\mathbf{r}) = j_\ell(qr)Y_{\ell m}(\Omega)H(a - r) \quad (2)$$

where  $j_\ell(x)$  is a spherical Bessel function of the first kind,  $Y_{\ell m}(\Omega)$  is a spherical harmonic and  $H(x)$  is the Heaviside step function.  $\ell$  and  $m$  are the usual quantum numbers for angular momentum, and the allowed values of  $q$  are determined by the boundary condition  $j_\ell(qa) = 0$ .  $\Omega$  denotes the pair of angular spherical polar coordinates  $(\vartheta, \varphi)$  of the point  $\mathbf{r}$ .

It is anticipated that in a practical calculation overlapping spherical regions  $\alpha$  of radius  $a_\alpha$  will be centred on each atom at position  $\mathbf{R}_\alpha$ , containing basis functions denoted by

$$\chi_{\alpha,n\ell m}(\mathbf{r} - \mathbf{R}_\alpha) = j_\ell(q_{\alpha,n\ell} |\mathbf{r} - \mathbf{R}_\alpha|) Y_{\ell m}(\Omega_{\mathbf{r}-\mathbf{R}_\alpha}) H(a_\alpha - |\mathbf{r} - \mathbf{R}_\alpha|). \quad (3)$$

Here  $n$  is the principal quantum number that labels the allowed values of  $q$  for a given  $\ell$ :  $q_{\alpha,n\ell}$  is the  $n$ -th root of the equation  $j_\ell(qa_\alpha) = 0$ .

The energy of such a localised spherical-wave is  $E_{\alpha,n\ell m} = q_{\alpha,n\ell}^2$  and so as for plane-waves this basis set may be truncated by including only those functions with energies less than  $E_{\text{cut}}$ . This condition also specifies a cut-off on the angular momentum of the basis  $\ell_{\text{cut},\alpha}$  in sphere  $\alpha$  but sometimes it is desirable to impose an independent global limit  $\ell_{\text{max}}$ .

### 3. Two-centre integrals

Two-centre integrals required for any electronic structure calculation include the overlap and kinetic energy matrices. The latter can be particularly difficult to evaluate accurately in the case of orbitals that are localised in space. By way of example, consider the overlap matrix elements between two basis functions, where the composite indices  $A \equiv \{\alpha, n\ell m\}$  and  $B \equiv \{\beta, n'\ell' m'\}$  have been introduced:

$$S_{AB} = \int_{\text{all space}} \chi_A^*(\mathbf{r} - \mathbf{R}_\alpha) \chi_B(\mathbf{r} - \mathbf{R}_\beta) d^3r. \quad (4)$$

Following [13] this is identified as a cross-correlation which can be evaluated using the Fourier transform of the basis functions given in (A.1):

$$S_{AB} = q_A a_\alpha^2 j_{\ell-1}(q_A a_\alpha) q_B a_\beta^2 j_{\ell'-1}(q_B a_\beta) I_{AB} \quad (5)$$

where the integral

$$I_{AB} = 8 \sum_{\lambda=0}^{\infty} \sum_{\mu=-\lambda}^{\lambda} i^{\lambda-\ell+\ell'} Y_{\lambda\mu}^*(\Omega_{\mathbf{R}_{\alpha\beta}}) \int Y_{\ell m}^*(\Omega_{\mathbf{k}}) Y_{\ell' m'}(\Omega_{\mathbf{k}}) Y_{\lambda\mu}(\Omega_{\mathbf{k}}) d\Omega_{\mathbf{k}} \\ \times \int_0^\infty \frac{j_\ell(ka_\alpha) j_{\ell'}(ka_\beta) j_\lambda(kR_{\alpha\beta})}{(k^2 - q_A^2)(k^2 - q_B^2)} k^2 dk \quad (6)$$

and  $\mathbf{R}_{\alpha\beta} = \mathbf{R}_\beta - \mathbf{R}_\alpha$ . Talman [17] has generalised this Fourier transform-based approach to numerical basis sets.

At this point the analysis departs from [13] and the angular integral is written as a Clebsch-Gordan coefficient. It is non-zero only for  $|\ell - \ell'| \leq \lambda \leq \ell + \ell'$ ,  $L = \ell + \ell' + \lambda$  even, and  $\mu = m - m'$ , simplifying the sums in (6).

For the radial integral consider the expansion of the spherical Bessel functions in terms of spherical Hankel functions as given in (A.3). As the integrand is even, the integration limits are expanded to yield:

$$J_{AB,\lambda\mu} = \frac{1}{2} \int_{-\infty}^{\infty} \frac{k^2}{(k^2 - q_A^2)(k^2 - q_B^2)} \left[ h_\ell^{(1)}(ka_\alpha) + h_\ell^{(2)}(ka_\alpha) \right] \left[ h_{\ell'}^{(1)}(ka_\beta) + h_{\ell'}^{(2)}(ka_\beta) \right] \\ \times \left[ h_\lambda^{(1)}(kR_{\alpha\beta}) + h_\lambda^{(2)}(kR_{\alpha\beta}) \right] dk. \quad (7)$$

This integral may be evaluated using the calculus of residues by writing it as a contour integral for complex  $k$  that runs along the real axis and is closed in the upper or lower half-plane as appropriate. Except for the case  $\ell = \ell' = \lambda$ , there is a higher order pole at the origin  $k = 0$ . Extra terms may be added to regularise the integral which cancel when all of the contributions are summed. The contribution from the resulting simple pole at  $k = 0$  is:

$$J_{AB,\lambda\mu}^{(0)} = \frac{(-1)^{L/2} \pi (2\ell)! (2\ell')! (2\lambda)!}{2^{L+1} \ell! \ell'! \lambda! L! q_A^2 a_\alpha^{\ell+1} q_B^2 a_\beta^{\ell'+1} R_{\alpha\beta}^{\lambda+1}} \left[ -\text{sgn}(a_\alpha + a_\beta + R_{\alpha\beta})(a_\alpha + a_\beta + R_{\alpha\beta})^L \right. \\ \left. + \text{sgn}(a_\alpha + a_\beta - R_{\alpha\beta})(a_\alpha + a_\beta - R_{\alpha\beta})^L + \text{sgn}(a_\alpha - a_\beta + R_{\alpha\beta})(a_\alpha - a_\beta + R_{\alpha\beta})^L \right. \\ \left. + \text{sgn}(-a_\alpha + a_\beta + R_{\alpha\beta})(-a_\alpha + a_\beta + R_{\alpha\beta})^L \right] \quad (8)$$

Defining  $h^{(+)} \equiv h^{(1)}$  and  $h^{(-)} \equiv h^{(2)}$ , the contributions from each of the remaining four simple poles (at  $k = \pm q_A$  and  $k = \pm q_B$ ) are divided into eight terms  $J_{\pm\pm\pm\pm}^{(k)}$ , where the subscript indicates the kind of spherical Hankel functions in the order they appear in (7). Also defining  $R_{\pm\pm\pm\pm} = \pm a_\alpha \pm a_\beta \pm R_{\alpha\beta}$ , the poles at  $k = \pm q_A$  together contribute

$$J_{\pm\pm\pm\pm}^{(\pm q_A)} = \frac{i\pi q_A}{2(q_A^2 - q_B^2)} \\ \times \left[ \left( 1 - e^{-iq_A R_{\pm\pm\pm\pm}} \sum_{s=0}^{L-1} \frac{(iq_A R_{\pm\pm\pm\pm})^s}{s!} \right) \text{sgn}(R_{\pm\pm\pm\pm}) h_\ell^{(\pm)}(q_A a_\alpha) h_{\ell'}^{(\pm)}(q_A a_\beta) h_\lambda^{(\pm)}(q_A R_{\alpha\beta}) \right. \\ \left. - \left( 1 - e^{iq_A R_{\pm\pm\pm\pm}} \sum_{s=0}^{L-1} \frac{(-iq_A R_{\pm\pm\pm\pm})^s}{s!} \right) \text{sgn}(R_{\pm\pm\pm\pm}) h_\ell^{(\mp)}(q_A a_\alpha) h_{\ell'}^{(\mp)}(q_A a_\beta) h_\lambda^{(\mp)}(q_A R_{\alpha\beta}) \right] \quad (9)$$

with a similar expression for  $\pm q_B$ , obtained by exchanging  $q_A \leftrightarrow q_B$ . The radial integral is obtained by summing up all contributions for all poles.

Note that for  $R_{\alpha\beta} \geq a_\alpha + a_\beta$  the overlap integral must vanish. This fact is not obvious from the above expressions, but arises from complete cancellation between all of the contributions.

The kinetic energy matrix elements may be obtained in a similar manner

$$T_{AB} = - \int_{\text{all space}} \chi_A^*(\mathbf{r} - \mathbf{R}_\alpha) \nabla^2 \chi_B(\mathbf{r} - \mathbf{R}_\beta) d^3r \quad (10)$$

which simply introduces a factor of  $k^2$  into the radial integral of (6). The same analysis can be made except (i) the sums over  $s$  in (9) run only up to  $L - 3$ , (ii) an extra factor  $q_A^2$  or  $q_B^2$  occurs in (9) for the contributions from the poles at  $\pm q_A$  and  $\pm q_B$  respectively, (iii) the integrand in (7) only has a pole at  $k = 0$  when  $L \geq 2$ .

#### 4. Projection of basis functions

Consider the projection of a function centred in its own “home” sphere into a different “host” sphere centred elsewhere as illustrated in figure 1. The evaluation of the overlap integral then becomes trivial. This method is based on the one described in [13], but includes a contribution from the discontinuity in the first derivative of the basis functions at the boundary of the sphere that proves to be crucial.

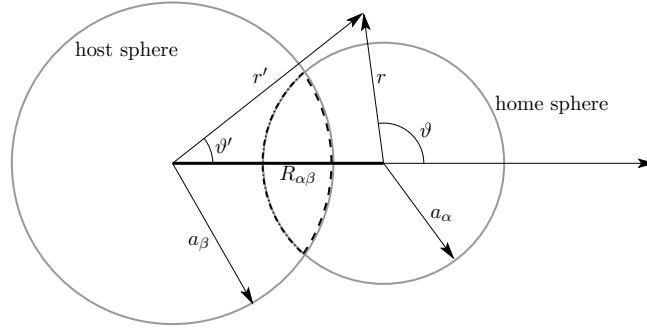


**Figure 1.** Diagram of home and host spheres with coordinate systems defined on each. - - - indicates the surface on which  $f$  is evaluated, — · — indicates the surface on which  $d$  is evaluated.

The basis functions are of the form given by (3), and direct substitution into the Helmholtz equation (1) yields, after some manipulation that exploits the fact that the right-hand side vanishes except at the boundary of the sphere  $r = a_\alpha$ ,

$$(\nabla^2 + q_A^2)\chi_A(\mathbf{r}) = -Y_{\ell m}(\Omega) \delta(a_\alpha - r) q_A j_{\ell-1}(q_A r) \equiv d_A(\mathbf{r}). \quad (11)$$

The sphere  $\alpha$  is called the “home” region of  $\chi_A$  and is taken to be centred on the origin. Consider a second “host” sphere  $\beta$  which contains its own set of basis functions  $\{\chi_B\}$ . The projection requires the expansion of  $\chi_A$  in terms of the  $\{\chi_B\}$  i.e. from the home to the host sphere. As in [13], the uniqueness theorem for the Helmholtz equation is invoked which means that the projected function is uniquely determined by the boundary conditions on the surface of the host region. The inhomogeneous Helmholtz equation (11) may be solved using the formal expansion of the Green’s function subject to the inhomogeneous boundary conditions arising from the fact that  $\chi_A$  will not in general vanish on the surface of the host sphere:

$$\chi_A(r' = a_\beta) = \chi_A(|\mathbf{r} - \mathbf{R}_{\alpha\beta}| = a_\beta) \equiv f_A(\Omega). \quad (12)$$

Unprimed coordinates refer to the home sphere  $\alpha$  while primed coordinates refer to the host sphere  $\beta$  and are measured with respect to  $\mathbf{R}_\beta$ . The solution of (11) subject to the boundary conditions (12) is required. First, the boundary conditions are made homogeneous by introducing the function

$$\eta_A(\mathbf{r}) = \chi_A(\mathbf{r}) - f_A(\Omega). \quad (13)$$

The functions  $\eta_A$ ,  $d_A$  and  $f_A$  are now decomposed into the angular momentum components of the *host* sphere e.g.

$$\eta_{A,\ell'm'}(r') = \int Y_{\ell'm'}^*(\Omega') \eta_A(\mathbf{r}' + \mathbf{R}_{\alpha\beta}) d\Omega' \quad (14)$$

reducing the problem to a set of radial differential equations:

$$\begin{aligned} & \left[ \frac{1}{r'^2} \frac{d}{dr'} \left( r'^2 \frac{d}{dr'} \right) + q_A^2 - \frac{\ell'(\ell'+1)}{r'^2} \right] \eta_{A,\ell'm'}(r') \\ & = d_{A,\ell'm'}(r') + \frac{\ell'(\ell'+1)}{r'^2} f_{A,\ell'm'} - q_A^2 f_{A,\ell'm'}. \end{aligned} \quad (15)$$

Next, the homogeneous equation is solved to obtain the normalised eigenfunctions used to determine the Green's function  $G(r', r'')$  given by

$$G(r', r'') = \sum_{n'=1}^{\infty} \frac{j_{\ell'}(q_B r') j_{\ell'}(q_B r'')}{\left[ \frac{1}{2} a_{\beta}^3 j_{\ell'-1}^2(q_B a_{\beta}) \right] (q_A^2 - q_B^2)}. \quad (16)$$

This leads to a particular integral for (15) of the form

$$\int_0^{a_{\beta}} \left[ d_{A,\ell'm'}(r'') + \left( \frac{\ell'(\ell'+1)}{r''^2} - q_A^2 \right) f_{A,\ell'm'} \right] G(r', r'') r''^2 dr''. \quad (17)$$

The evaluation of  $d_{A,\ell'm'}$  is straightforward, yielding

$$\begin{aligned} d_{A,\ell'm'}(r') & = -\frac{q_A a_{\alpha} j_{\ell-1}(q_A a_{\alpha})}{2 R_{\alpha\beta} r'} \sqrt{(2\ell+1)(2\ell'+1) \frac{(\ell-m)! (\ell'-m)!}{(\ell+m)! (\ell'+m)!}} \\ & \times P_{\ell'}^{m'} \left( \frac{r'^2 + R_{\alpha\beta}^2 - a_{\alpha}^2}{2 R_{\alpha\beta} r'} \right) P_{\ell}^m \left( \frac{r'^2 - R_{\alpha\beta}^2 - a_{\alpha}^2}{2 R_{\alpha\beta} a_{\alpha}} \right), \end{aligned} \quad (18)$$

where we have assumed that the vector  $\mathbf{R}_{\alpha\beta}$  joining the centres lies along the  $z$ -axis. If that were not the case, a simple coordinate rotation that mixes the spherical harmonics is necessary. In this configuration the host and home coordinate systems are simply related. Since  $\vartheta'$  is constrained to describe points on the surface of  $\alpha$  that lie inside  $\beta$ ,  $|R_{\alpha\beta} - a_{\alpha}| \leq r' \leq \min(R_{\alpha\beta} + a_{\alpha}, a_{\beta})$ , corresponding to the values of  $r'$  for which the associated Legendre polynomials are real-valued.

The integral  $f_{A,\ell'm'}$  has a similar form to that part of (17) involving  $d_{A,\ell'm'}$ , and a general method for its evaluation is presented in Appendix B. These results can now be used to calculate the overlap integral  $S_{AB}$  by projecting  $\chi_A$  into  $\beta$

$$\chi_{A \rightarrow \beta}(\mathbf{r}') = \sum_{\ell'=0}^{\infty} \sum_{m'=-\ell'}^{\ell'} (\eta_{A,\ell'm'}(r') + f_{A,\ell'm'}) Y_{\ell'm'}(\Omega'), \quad (19)$$

where  $\chi_{A \rightarrow \beta} \neq \chi_A$  as the basis set in  $\beta$  is not complete – for example  $\chi_{A \rightarrow \beta}$  vanishes over the surface of  $\beta$  whereas  $\chi_A$  does not in general.  $\chi_{A \rightarrow \beta}$  is the closest function to  $\chi_A$  in a least-squares sense for points  $\mathbf{r}$  in  $\beta$ .  $S_{AB}$  is then given by

$$\begin{aligned}
 S_{AB} &= \frac{f_{A,\ell'm'}}{q_A^2 - q_B^2} \int_0^{a_\beta} r'^2 \left( \frac{\ell'(\ell'+1)}{r'^2} - q_B^2 \right) j_{\ell'}(q_B r') \, dr' \\
 &\quad + \frac{1}{q_A^2 - q_B^2} \int_{|R_{\alpha\beta} - a_\alpha|}^{\min(R_{\alpha\beta} + a_\alpha, a_\beta)} r'^2 j_{\ell'}(q_B r') \, d_{A,\ell'm'}(r') \, dr'
 \end{aligned} \tag{20}$$

where the integral involving  $d_{A,\ell'm'}$  is of the same form as (B.1).

In order to evaluate the kinetic energy matrix elements, consider

$$\begin{aligned}
 T_{AB} &= - \int_{\text{all space}} \chi_A^*(\mathbf{r}) \nabla'^2 \chi_B(\mathbf{r}') \, d^3 r' = \int_{\text{all space}} \chi_A^*(\mathbf{r}) \left[ q_B^2 \chi_B(\mathbf{r}') - d_B(\mathbf{r}') \right] \, d^3 r' \\
 &= q_B^2 S_{AB} - \int_{\text{all space}} \chi_A^*(\mathbf{r}) d_B(\mathbf{r}') \, d^3 r'.
 \end{aligned} \tag{21}$$

The second term may be calculated by projecting  $\chi_A(\mathbf{r})$  into  $\beta$  leading to a particularly simple form for the kinetic energy matrix elements:

$$T_{AB} = q_B^2 S_{AB} + q_B a_\beta^2 j_{\ell'-1}(q_B a_\beta) f_{A,\ell'm'} = q_A^2 S_{AB} + q_A a_\alpha^2 j_{\ell-1}(q_A a_\alpha) f_{B,\ell m}. \tag{22}$$

## 5. Results and scaling

### 5.1. Accuracy

In this section both overlap and kinetic energy matrix elements calculated using both methods above are compared with numerical results. In all examples  $a_\alpha = 3$  and  $a_\beta = 4$  arbitrary units. For the numerical evaluation of the kinetic energy the symmetric form

$$T_{AB} = \int_{\text{all space}} \nabla \chi_A^*(\mathbf{r} - \mathbf{R}_\alpha) \cdot \nabla \chi_B(\mathbf{r} - \mathbf{R}_\beta) \, d^3 r \tag{23}$$

is used with the gradients calculated by finite differences.

Figure 2 shows the variation of the overlap matrix elements between selected basis functions as a function of separation. The matrix element vanishes correctly when  $R_{\alpha\beta} \geq a_\alpha + a_\beta$ .

Figure 3 shows the variation in kinetic energy matrix elements for the same selection of basis functions as in figure 2. The fact that the overlap and kinetic energy matrix elements are clearly not proportional highlights the contribution arising from the discontinuity of the basis functions at the sphere boundaries.

From these plots it is clear that the analytic results from both methods are both in generally good agreement with the numerical estimate, with some differences, most notably in figure 3(c) attributed to the difficulty of accurately calculating kinetic energies of localised functions by finite differences [18].

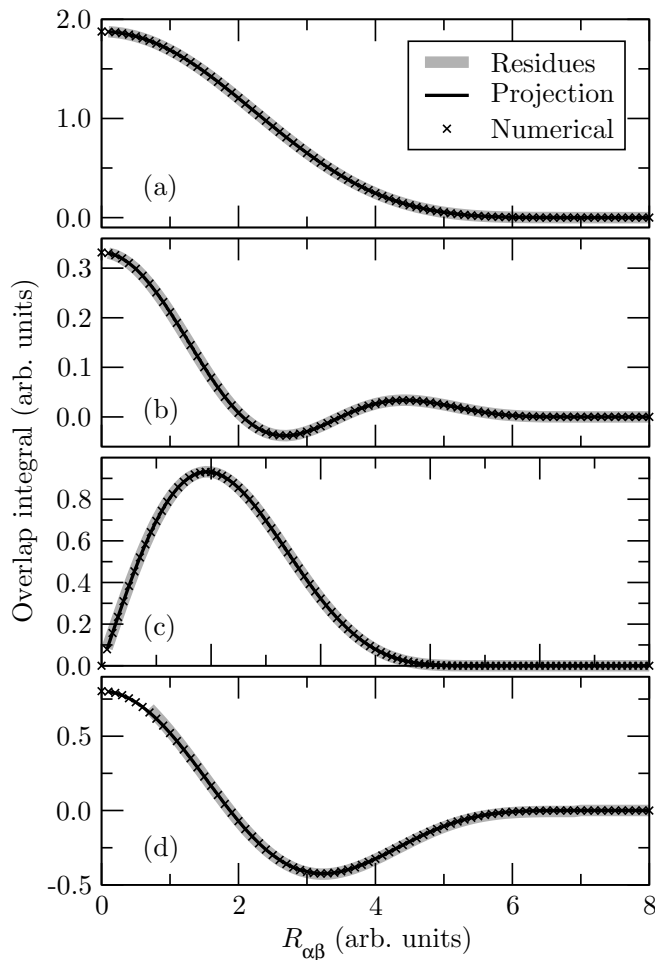


**Figure 2.** Overlap integrals as a function of the centre separation  $R_{\alpha\beta}$  using the residue, projection and numerical methods. (a)  $\ell = \ell' = 0$  and  $n = n' = 1$ . (b)  $\ell = \ell' = 0$  and  $n = n' = 2$ . (c)  $\ell = 0, \ell' = 1$  and  $n = n' = 1$ . (d)  $\ell = \ell' = 1$  and  $n = n' = 1$ .

### 5.2. Scaling

For simplicity assume that the maximum angular momentum component for all spheres is  $\ell_{\max}$ . The size of the basis set increases as  $(\ell_{\max} + 1)^2$  and hence the number of matrix elements to be calculated scales asymptotically as  $\ell_{\max}^4$ .

For a single matrix element calculated using the calculus of residues as in section 3, the computational effort is dominated by the sums over  $s$  in 9. Together with the sum over  $\lambda$  from the expansion of  $\exp(i\mathbf{k} \cdot \mathbf{R}_{\alpha\beta})$  this yields a theoretical computational cost for the worst case matrix element that scales as  $\ell_{\max}^2$ . Evaluation of the spherical Hankel functions  $h^{(1)}(x)$  and  $h^{(2)}(x)$  using Lentz's method for continued fractions would introduce another factor of  $\ell_{\max}$  to the scaling, but a cubic spline can be fitted to avoid this. Overall the construction of the overlap and kinetic energy matrices scales as  $\ell_{\max}^6$ .

For the projection method in section 4, in the evaluation of both  $f_{A,\ell'm'}$  and  $d_{A,\ell'm'}$  there appear a number of sums which dominate the calculation. For the worst case

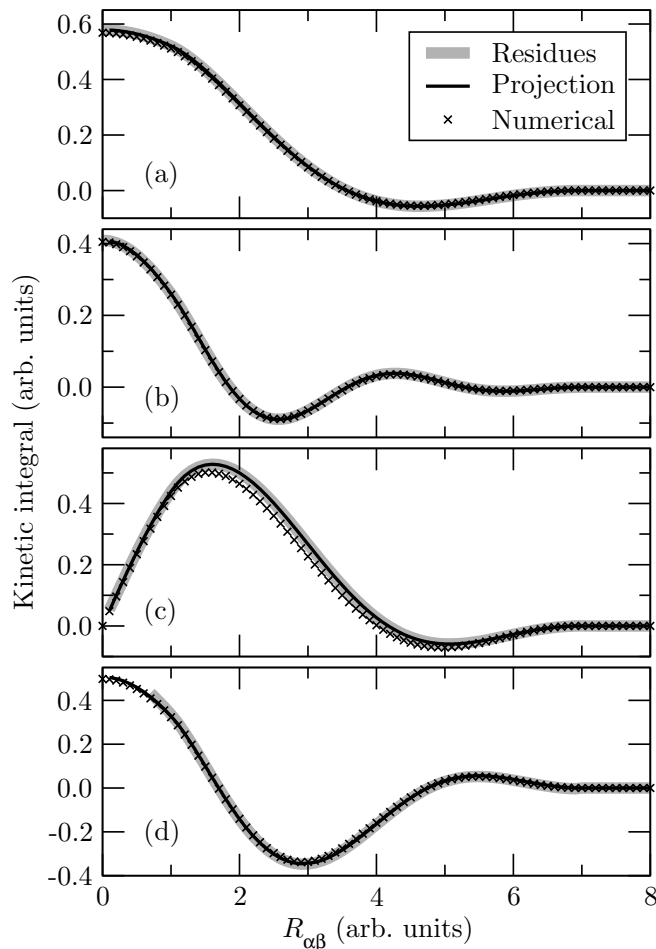


**Figure 3.** Kinetic integrals as a function of the centre separation  $R_{\alpha\beta}$  using the residue, projection and numerical methods. (a)  $\ell = \ell' = 0$  and  $n = n' = 1$ . (b)  $\ell = \ell' = 0$  and  $n = n' = 2$ . (c)  $\ell = 0, \ell' = 1$  and  $n = n' = 1$ . (d)  $\ell = \ell' = 1$  and  $n = n' = 1$ .

( $m = 0$ ) the calculation of a single matrix element scales as  $\ell_{\max}^6$  and this determines the overall scaling of  $\ell_{\max}^{10}$ . The asymptotic scaling of both methods is confirmed by the results shown in the main graph of figure 4.

In [13] the two-centre integrals were calculated by performing  $\ell + \ell'$  derivatives of a radial integral, a method which potentially scales exponentially with  $\ell_{\max}$  unless the majority of terms can be combined or cancel. Both methods derived here scale favourably compared to that approach. The inset of figure 4 shows the speedup obtained with a straightforward implementation of both methods proposed here relative to the original optimised code based on the approach of [13] for small values of  $\ell$ . In spite of the poorer asymptotic scaling, the smaller prefactor of the projection method suggests that it may be the preferred approach for practical calculations where reasonable accuracy may be obtained with  $\ell_{\max} = 3$  as shown previously [14, 15].

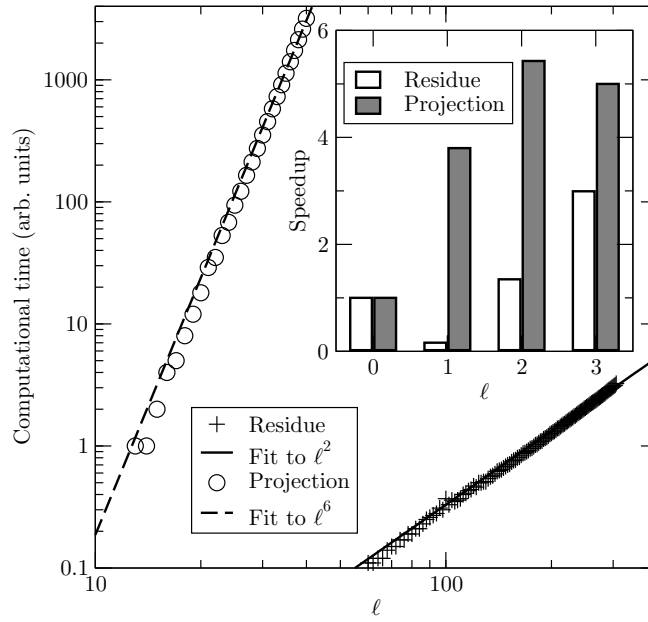


**Figure 4.** Logarithmic plot of computational time against  $\ell = \ell'$  for the evaluation of a single overlap matrix element. The residue method scales as a power of 2 while the projection method scales as a power of 6. Inset: speedup of both methods proposed here compared to the original scheme of [13] for small  $\ell$ .

## 6. Three-centre integrals

The projection method can of course be carried out more efficiently by using the overlap matrix elements obtained from the first method. Write (19) in the form

$$\chi_{A \rightarrow \beta}(\mathbf{r}') = \sum_{\nu\lambda\mu} C_{\nu\lambda\mu} \chi_{\beta,\nu\lambda\mu}(\mathbf{r}') \quad (24)$$

and therefore using the orthogonality of the basis functions in  $\beta$ :

$$S_{AB} = \frac{1}{2} a_\beta^3 j_{\ell'-1}^2(q_B a_\beta) C_{n'\ell'm'} \Rightarrow C_{n'\ell'm'} = \frac{2S_{AB}}{a_\beta^3 j_{\ell'-1}^2(q_B a_\beta)}. \quad (25)$$

Now consider a three-centre integral such as the non-local pseudopotential from a single atom in semi-local form:

$$\hat{V}_{\text{NL}} = \sum_{\lambda\mu} |Y_{\lambda\mu}\rangle V_\lambda(r'') \langle Y_{\lambda\mu}| \quad (26)$$

where the spherical harmonics are centred on the atom,  $r''$  is the distance from the atom and  $V_\lambda(r'')$  vanishes beyond the core radius i.e. for  $r'' \geq a_c$ .  $V_\lambda$  may thus be expanded in spherical Bessel functions within the core i.e.

$$\begin{aligned} V_\lambda(r'') &= \sum_{\nu=1}^{\infty} V_{\nu\lambda} j_\nu(q_{c,\nu\lambda} r'') \\ \Rightarrow V_{\nu\lambda} &= \frac{2}{a_c^3 j_{\lambda-1}^2(q_{c,\nu\lambda} a_c)} \int_0^{a_c} V_\lambda(r'') j_\nu(q_{c,\nu\lambda} r'') r''^2 dr'' \end{aligned} \quad (27)$$

where  $q_{c,\nu\lambda}$  satisfies  $j_\lambda(q_{c,\nu\lambda}a_c) = 0$ .

Introducing the composite index  $C \equiv \{c, \nu\lambda\mu\}$  to label a spherical-wave basis in the core,

$$\hat{V}_{\text{NL}} = \sum_{\nu\nu'\lambda\mu} |\chi_C\rangle V_{\nu\nu'\lambda} \langle\chi_{C'}| \quad (28)$$

where

$$V_{\nu\nu'\lambda} = \frac{\langle\chi_C|\hat{V}_{\text{NL}}|\chi_{C'}\rangle}{\langle\chi_C|\chi_C\rangle\langle\chi_{C'}|\chi_{C'}\rangle} \quad (29)$$

Hence

$$\hat{V}_{\text{NL},AB} = \sum_{\nu\nu'\lambda\mu} S_{AC} V_{\nu\nu'\lambda} S_{CB} \quad (30)$$

reducing a three-centre integral to a sum of products of two-centre integrals. Exactly the same result may be obtained by projecting  $\chi_A$  and  $\chi_B$  onto the core sphere and then performing a one-centre integral.

## 7. Conclusions

Two analytical methods for the evaluation of overlap matrix elements between localised spherical-wave basis functions have been presented. Both methods may be extended straightforwardly to the evaluation of the kinetic energy matrix elements. The complexity of three-centre integrals can be significantly reduced. The results for the two methods agree with each other and numerical integration.

The method that uses the calculus of residues is more efficient computationally (if less elegant) than the projection method, but both are more efficient than the method originally proposed.

## Acknowledgments

PDH acknowledges the support of a Royal Society University Research Fellowship.

## Appendix A. Standard results

This appendix lists published results [13, 19] used in the analysis in this paper.

The Fourier transform of a basis function  $\chi_A$  is given by

$$\tilde{\chi}_A(\mathbf{k}) = 4\pi i^\ell Y_{\ell m}(\Omega_{\mathbf{k}}) \int_0^{a_\alpha} j_\ell(qr) j_\ell(kr) r^2 dr \quad (\text{A.1})$$

and the cross-correlation form of the overlap matrix involves

$$I_{AB} = \frac{(2i)^{\ell-\ell'}}{\pi} \int e^{-i\mathbf{k}\cdot\mathbf{R}_{\alpha\beta}} \frac{j_\ell(ka_\alpha) j_{\ell'}(ka_\beta)}{(k^2 - q_A^2)(k^2 - q_B^2)} Y_{\ell m}^*(\Omega_{\mathbf{k}}) Y_{\ell' m'}(\Omega_{\mathbf{k}}) d^3k. \quad (\text{A.2})$$

The spherical Bessel function can be expanded in terms of the spherical Hankel functions of first and second kind,  $h_\ell^{(1)}$  and  $h_\ell^{(2)}$  respectively, according to

$$j_\ell(z) = \frac{1}{2} \left[ h_\ell^{(1)}(z) + h_\ell^{(2)}(z) \right]. \quad (\text{A.3})$$

Also, the Hankel function of the first kind can be represented as

$$h_\ell^{(1)}(z) = (-i)^{\ell+1} \frac{e^{iz}}{z} \sum_{s=0}^{\ell} \frac{i^s}{s! (2z)^s} \frac{(\ell+s)!}{(\ell-s)!}, \quad (\text{A.4})$$

and for real argument  $h_\ell^{(2)}(z) = h_\ell^{(1)*}(z)$ .

## Appendix B. Integral evaluation

The integral  $f_{A,\ell'm'}$  has a similar form to that part of (17) involving  $d_{A,\ell'm'}$ :

$$f_{A,\ell'm'} = \int_{|1-u|}^v P_{\ell'}^{m'} \left( \frac{1+u^2-z^2}{2u} \right) P_\ell^m \left( \frac{1-u^2-z^2}{2uz} \right) j_\ell(q_A a_\beta z) z dz, \quad (\text{B.1})$$

where  $u = R_{\alpha\beta}/a_\beta$ ,  $v = a_\alpha/a_\beta$  and  $z = \sqrt{1+u^2-2u \cos \vartheta'}$ , and the integral

$$\int_{|R_{\alpha\beta}-a_\alpha|}^{\min(R_{\alpha\beta}+a_\alpha, a_\beta)} P_{\ell'}^{m'} \left( \frac{r^2+R_{\alpha\beta}^2-a_\alpha^2}{2R_{\alpha\beta}r} \right) P_\ell^m \left( \frac{r^2-R_{\alpha\beta}^2-a_\alpha^2}{2R_{\alpha\beta}a_\alpha} \right) j_\ell(q_B r) r dr, \quad (\text{B.2})$$

where prefactors have been omitted in both expressions. Again, it has been assumed that the  $z$ -axis is aligned with  $\mathbf{R}_{\alpha\beta}$  so that the  $\varphi'$  integral yields  $2\pi\delta_{mm'}$ . The evaluation of  $f_{A,\ell'm'}$  is used as an example with final solution:

$$\begin{aligned} f_{A,\ell'm'} &= \frac{1}{2q_A R_{\alpha\beta}} \left( \frac{a_\beta}{2R_{\alpha\beta}} \right)^{\ell+\ell'} \sqrt{(2\ell+1)(2\ell'+1) \frac{(\ell-m)! (\ell'-m)!}{(\ell+m)! (\ell'+m)!}} \\ &\times \sum_{p=0}^{[(\ell-m)/2]} c_{\ell m}^{(p)} \sum_{k=0}^{\ell-m-2p} \binom{\ell-m-2p}{k} \sum_{p'=0}^{[(\ell'-m)/2]} c_{\ell' m}^{(p')} \sum_{k'=0}^{\ell'-m-2p'} \binom{\ell'-m-2p'}{k'} \\ &\times \sum_{k''=0}^{m+p+p'} \binom{m+p+p'}{k''} \sum_{k'''=0}^{m+p+p'} \binom{m+p+p'}{k'''} (-1)^K \\ &\times (1-u^2)^{\ell-m-2p-k} (1+u^2)^{\ell'-m-2p'-k'} (1+u)^{2(m+p+p'-k'')} (1-u)^{2(m+p+p'-k''')} \\ &\times \left\{ \sum_{s=0}^{[\ell/2]} \frac{(-1)^s (\ell+2s)!}{(2s)! (\ell-2s+1)! (2q_A a_\beta)^{2s}} \int_{|u-1|}^v z^{-\ell+2(K-s)} \sin \left( q_A a_\beta z - \frac{\pi\ell}{2} \right) dz \right. \\ &\left. + \sum_{s=0}^{[(\ell-1)/2]} \frac{(-1)^s (\ell+2s+1)!}{(2s+1)! (\ell-2s)! (2q_A a_\beta)^{2s+1}} \int_{|u-1|}^v z^{-\ell-1+2(K-s)} \cos \left( q_A a_\beta z - \frac{\pi\ell}{2} \right) dz \right\}, \quad (\text{B.3}) \end{aligned}$$

where  $K = k + k' + k'' + k'''$  and the expression given in [20] for the associated Legendre polynomial with the corresponding notation is used, and the expression used for the spherical Bessel functions is:

$$j_\ell(z) = \frac{1}{z} \left\{ \sum_{k=0}^{\lfloor \ell/2 \rfloor} \frac{(-1)^k (\ell + 2k)!}{(2k)! \Gamma(\ell - 2k + 1) (2z)^{2k}} \sin \left( z - \frac{\pi \ell}{2} \right) + \sum_{k=0}^{\lfloor (\ell-1)/2 \rfloor} \frac{(-1)^k (\ell + 2k + 1)!}{(2k + 1)! \Gamma(\ell - 2k) (2z)^{2k+1}} \cos \left( z - \frac{\pi \ell}{2} \right) \right\}. \quad (\text{B.4})$$

The last two integrals have argument sine or cosine times an integer power, with trivial solution. If the integer power is negative, the expressions result in sine or cosine integrals, but the limits are such that no convergence problems arise.

## References

- [1] Payne M C, Teter M P, Allan D C, Arias T A and Joannopoulos J D 1992 *Rev. Mod. Phys.* **64** 1045–97
- [2] Goedecker S 1999 *Rev. Mod. Phys.* **71** 1085–1123
- [3] Brouder C, Panati G, Calandra M, Mourougane C and Marzari N 2007 *Phys. Rev. Lett.* **98**, 046402
- [4] Mostofi A A, Haynes P D, Skylaris C-K and Payne M C 2003 *J. Chem. Phys.* **119**, 8842–8 (2003)
- [5] Skylaris C-K, Mostofi A A, Haynes P D, Diéguez O and Payne M C 2002 *Phys. Rev. B* **66** 035119
- [6] Skylaris C-K and Haynes P D 2007 *J. Chem. Phys.* **127** 164712
- [7] Davidson E R and Feller D 1986 *Chem. Rev.* **86** 681–96
- [8] Guerra C F, Snijders J G, te Velde G and Baerends E J 1998 *Theor. Chem. Acc.* **99** 391–403
- [9] Junquera J, Paz O, Sánchez-Portal D and Artacho E 2001 *Phys. Rev. B* **64** 235111
- [10] Hernández E, Gillan M J and Goringe C M 1997 *Phys. Rev. B* **55** 13485–93
- [11] Varga K, Zhang Z and Pantelides S T 2004 *Phys. Rev. Lett.* **93** 176403
- [12] Beck T L 2000 *Rev. Mod. Phys.* **72** 1041–80
- [13] Haynes P D and Payne M C 1997 *Comput. Phys. Commun.* **102** 17–27
- [14] Gan C K, Haynes P D and Payne M C 2001 *Phys. Rev. B* **63** 205109
- [15] Haynes P D and Payne M C 1999 *Phys. Rev. B* **59** 12173–6
- [16] Kleinman L and Bylander D M 1982 *Phys. Rev. Lett.* **48**, 1425–8
- [17] Talman J D 2003 *J. Quantum Chem.* **93** 72–90
- [18] Skylaris C-K, Diéguez O, Haynes P D and Payne M C 2002 *Phys. Rev. B* **66** 073103
- [19] Abramowitz M and Stegun I 1965 *Handbook of Mathematical Functions* (New York: Dover)
- [20] Wong B R 1998 *J. Phys. A: Math. Gen.* **31** 1101–3